# Topology of 1-pentagon carbon nanocones - Topological efficiency and magic sizes

Adhemar Bultheel* Ottorino Ori‡

**Abstract**

In this article topological modeling techniques have been applied to the study of one pentagon carbon nanocones (apical angle 19°) to derive important results about preferred sizes and chemical reactivity. This theoretical model looks to the nanocone just like a 3-connected graph and considers the topological efficiency (or topological roundness) of such a system as the longrange topological potential whose local minima correspond to magic sizes of the nanocone with high probability of formation. This study moreover shows that topology alone can determine a migration of the stable regions of the nanocone along the nanocone itself, leaving in such a way the apical pentagon in a topologically reactive status. This study expands and systematizes previous works on the same subject.

**Keywords:**Nanocones, Nanohorns, Topological Roundness, Topological Efficiency, Wiener weights

## 1 Introduction

Graphenic planar systems and hollow carbon nanostructures with hexagonal/pentagonal networks represent promising systems for innovative applications such as drug-carrying nanomachines, nanoelectronic and other devices. Electronic structures of 3-connected carbon systems like 1D nanotubes, 2D fullerenes and other 2D structures like carbon nanocones strongly depend on molecular topology and normally present atomically smooth surfaces. Here we focus on one-pentagon carbon nanocone (1P-CNC) whose inherent 2D dimensionality is derived, as a sort of topological signature, by the characteristics of its topological invariants.

CNC history began in 1994 [1] when they were observed in tunneling microscopy (STM) experiments as free-standing 19° cones with typical sizes of 24 nm in length and 8 nm in base diameter. Nowadays CNC are receiving renewed attention by the latest observations of these conical topologies under the name of carbon nanohorns (CNH), see [2]. CNC are in effect perfect

*Department of Computer Science, KU Leuven, Celestijnenlaan 200A, 3001 Heverlee, Belgium

†Actinium Chemical Research, 00133 Rome, Italy and Laboratory of Renewable Energies-Photovoltaics, National Institute for R&D in Electrochemistry and Condensed Matter IMCEMC-Timi soara, 300569 Timi soara, Romania

‡Corresponding author email ottorino.ori@gmail.com

structures to study the "nucleation and growth of curved carbon structures" [3] evidencing the pivotal role played by the pentagons in the atomic assembly mechanism. When one pentagon is placed into the honeycomb layer a disclination defect is then created in the graphenic plane leading to the formation of a conic structure with positive curvature in which the pentagon is surrounded by a first belt with 5 hexagons. Although this article is just devoted to the study of nanocones with one pentagon, it is worth to remind here that CNC's may contain up to 5 pentagons, the number of them influencing the opening angle of the nanocone assuming 19.2°, 38.9°, 60°, 86.6°, 123.6° discrete values. The $P = 6$ case corresponds to the cylindrical nanotubes and fullerenes with all possible "nanobarrel" variants [6]. As documented in the literature [3,4], the pentagons at the tip apex of the nanocone makes those carbon structures an analog of the ending cups of the carbon nanotubes (1D fullerenes [6]) whose electronical states show the peculiar presence of resonant peaks also observed in multiwall carbon nanotubes. A somehow heuristic argument [3] helps to clarify the effects played by the pentagonal rings at the apices of the nanocones on the local density of states that strongly depends on the "pentagon concentration and topology" of the pentagons dispersed in the hexagonal structure. The basic observation is that the $\pi$ electron states of an isolated 5-carbon ring shows an electronic affinity for a sixth electron in the bonding state. Therefore, as soon as the pentagon is surrounded by the $\pi$ electrons coming from the metallic hexagonal network, such a bonding state will be immediately occupied and screened by the other $\pi$ electrons, generating a resonant bonding state in the graphenic electronic structure. The bit of heuristics exposed above, allows us to imagine an electronic mechanism capable to compensate the distortions induced in the hexagonal carbon network by the pentagons by predicting the presence of stabilizing acceptor states in the apical region of the CNC. These states may be furtherly influenced by the interactions among different pentagonal defects, suggesting that these states may cover quite extended regions outside the pentagonal rings [3]. For 1P-CNC however the density of the electronic charge remains localized around the pentagon keeping also the fivefold symmetry of the nanocone topology. This fivefold feature of the electronic states will be also confirmed by the topological modeling simulations applied in the next section to the 1P-CNC case. In the relevant article [3] even accurate ab-initio energy values are reported, assigning to the resonant peaks for the nanocone with one pentagon an energy of $-0.6$ eV below the Fermi energy.

On the way towards the proper modeling of carbon nanocones as drug-nanocarrier, in the relevant study [4] the authors apply detailed DFT calculations to investigate the electronic and energetic features of CNC oxidized-forms. Oxidized "topologies" are in fact necessary in order to produce materials with advanced adsorption and releasing properties. The oxidizing mechanism, previously proposed for carbon nanotubes oxidation, exploits the presence of $O_2$ and $H_2O$ molecules leading to local formation of the carboxyl and hydroxyl groups in the region of the CNCox cap (see also articles [2] and related literature). The main discovery reported in [4] is about the presence of oxidized vacancies on the wall of the carbon structures. With the progress of the oxidation process large holes (with diameter up to 11 Å) in fact do appear on the CNC surface. The size of those holes are compatible with the dimensions of drugs like the cisplatin complex that occupies a sphere of approximately 0.5 nm radius, allowing in this way CNC to be considered as good candidates for drug-delivery nanomachines. The size of the CNC is therefore an important geometrical parameter that largely influences their chemical behavior. Measuring the CNC size with the number $f$ of hexagonal belts surrounding the CNC apex, the selected size for the CNC modeled in [4] is about

$f = 10$ whereas other studies [2,5] have reported values in the $f = 30$ range, corresponding to a length of about 50 nm. A complete, modern update about chemical properties and topological characteristics of CNC (or CNH) may be found in [2,7].

The present work presents an elegant application of the topological modeling (TM) method which describes a chemical system with $N$ atoms and $B$ bonds with a simple graph $G$ with $N$ vertices and $B$ edges and then considers the topological Hamiltonian governing the system like a linear composition $H^t(G) = \sum \Xi_k$ of suitable topological invariants computed on $G(N)$. The stable configurations of the system will be defined, as usual, by those configurations minimizing $H^t$. The scheme below summarizes the TM approach (long-range topological invariants will be described in the next paragraphs) being TM aim the one to sieve interesting configurations to be then analised in details by ab-initio tools.

Topological Modeling Sieve

Chemical system with $N$ atoms, $B$ bonds is described like a Graph with $N$ vertices, $B$ edges: $G(N, B)$

Energy of the system is described by combinations of Graph invariants[a]

$H^t(G) = \sum \Xi_k \quad \rightarrow \quad H^t(G)$ **local minima identify stable configurations of $G$ to be further investigated by ab-initio simulations.**

[a] Graph invariants of the form $\Xi_k(G) = \sum \tau_k^{ij}$ describe distance-based, long-range topological interactions between vertices pairs $(v_i, v_j)$. See next paragraphs.

TM has been applied in the last decade to $sp^2$ systems like schwarzitic junctions, fullerenes, benzenoid PAH systems and graphenic nanostructures with some relevant results [6, 8, 9, 11-13, 15, 16, 19, 20, 21] evidencing the TM ability to determine stable configurations of complex carbon networks. This paper will focus on the topological features of the 1P-CNC structure that is merely seen as 2D chemical graph with variable size $f$ (see Figure 1) governed by the topological potential that coincides with the topological efficiency $\rho$ of the structure, with the main goals of (i) reporting about TM analysis of the 1P-CNC structure; (ii) determining the actual nanocone sizes preferred by topology. The topological model not only defines those specific sizes but also predicts the increasing reactivity (loss of stability) of the pentagonal ring at the tip of the nanocones. In other words, the TM predicts an interesting property of 1P-CNC, namely that the topologically stable region of the carbon structure migrates during the CNC growth.

Present original results expand early topological studies reported in [8,9] and in the very detailed analyses given in the papers [11]. It is also necessary to remember here that the first pure topological studies on this subject have been proposed in 1994 [10], immediately after the CNC experimental discovery, under the correct assumption of treating those systems like "topological" defects of the graphite honeycomb mesh. This fact testifies the importance of building a topological description of the nanoworld to reach, the full understanding of the mutual interplay, rich of profound implications, between formal topological properties of cubic-graphs (graphs made by 3-connected vertices only) and real-world carbon chemistry.

Topological algorithms used in this work to analyze the 1P-CNC structures (in both direct and dual representations) are introduced in the next sections together with the main outcomes arising from the topological modeling. Comparison with previous topological investigations [8,9,11] will

be also provided.

## 2 Topological models for nanocones

This article follows the basic topological modeling approach looking at a chemical carbon structure with N atoms (like graphene or nanocones) just as a chemical cubic graph made by N nodes of valence 3. Despite this very basic approximation, interesting theoretical conclusions may be derived concerning the chemical relative stability and the probability of formation of such nanostructures. Figure 1a shows the 1P-CNC direct topology (graph $Z$) evidencing the first 5 atoms belonging to the pentagonal apex (with circles) and the one belonging to the first two belts of hexagons (black circles). The first belt $f = 1$ includes vertices labeled from 6 to 20, whereas the remaining 25 atoms belong to second circles of hexagons with $f = 2$. The 45 vertices shown in Figure 1a are labeled to provide some visual information about the topological symmetry of the $f = 2$ nanocone, for example the five white atoms belong to the pentagon are symmetric and the same holds for the five vertices $v_i$ with $i = 6, 7, 8, 9, 10$ forming another set of equivalent graph nodes that "bridge" the pentagon to the first belt of five hexagons. Other groups (orbits) of topologically equivalent atoms are visible in the structure, like the distinct sets of atoms $v_i$ with $i = 11, ..., 20$ and $v_i$ with $i = 21, ..., 25$ or the orbit made by the ten atoms $v_i$ with $i \in \{26, 27, 30, 31, 34, 35, 38, 39, 42, 43\}$ etc. The most effective and elegant way to expose the rich structural information (like for example to determine the orbits§, i.e. the sets of topologically equivalent atoms) is to make use of specific distance-based topological invariants computed for each vertex $v$ of the graph $G(N)$ ($N$ refers to the number of vertices in the graph). In this context the distance $d_{ij}$ between nodes $v_i$ and $v_j$ is simply the integer counting the minimal number of edges one must travel to reach atom $v_j$ starting from $v_i$ and vice versa. We focus on the set of integers $\{b_{ik}\}$ that count the number of atoms sitting in the $k$-coordination shells of $v_i$. Obviously $b_{i1}$ equals the number of bonds of atom $v_i$ with $b_{i1} = 3$ in the case of $sp^2$ carbon systems. If we denote by $M = \max\{d_{ij}\}$ the largest distance in the graph, we derive the useful normalization constraint:

$$N - 1 = \sum_{k=1}^{M} b_{ik}, \quad \forall i. \tag{1}$$

The complete topological information of the graph is stored in the set of Wiener-strings (WS) (see [8]) that is for all atoms $i$ in $G$ the set of strings $\{b_{ik}\}$. They are listed in Table 1. Based on these data, a new local invariant may be assigned to each node, the so-called Wiener-weight (WW):

$$w_i = \frac{1}{2} \sum_{k=1}^{M} k b_{ik}. \tag{2}$$

The local atomic invariants (2) are finally related to the Wiener index of the nanosystem. This is a global topological invariant defined by the summation:

$$W = \sum_{k=1}^{N} w_i. \tag{3}$$

| **a) Partitions (cardinality) of direct graph $Z_{f=2}$** | $\{b_{ik}\}$ | $w_i$ |
|---|---|---|
| $v_1$ $v_2$ $v_3$ $v_4$ $v_5$ (5) | 3 6 8 11 10 6 | 84.5 |
| $v_6$ $v_7$ $v_8$ $v_9$ $v_{10}$ (5) | 3 6 9 8 6 6 6 | 91.0 |
| $v_{11}$ $v_{12}$ $v_{13}$ $v_{14}$ $v_{15}$ $v_{16}$ $v_{17}$ $v_{18}$ $v_{19}$ $v_{20}$ (10) | 3 6 7 7 7 6 4 4 | 97.5 |
| $v_{26}$ $v_{27}$ $v_{30}$ $v_{31}$ $v_{34}$ $v_{35}$ $v_{38}$ $v_{39}$ $v_{42}$ $v_{43}$ (10) | 3 4 5 6 6 6 6 4 4 | 113.0 |
| $v_{21}$ $v_{22}$ $v_{23}$ $v_{24}$ $v_{25}$ (5) | 2 4 5 5 6 6 6 6 2 2 | 119.5 |
| $v_{28}$ $v_{29}$ $v_{32}$ $v_{33}$ $v_{36}$ $v_{37}$ $v_{40}$ $v_{41}$ $v_{44}$ $v_{45}$ (10) | 2 3 4 5 6 6 5 5 4 4 | 128.5 |
| **b) Partitions (cardinality) of dual graph $Z^*_{f=2}$** | $\{b_{ik}\}$ | $w_i$ |
| $v_1$ (1) | 5 10 | 12.5 |
| $v_2$ $v_3$ $v_4$ $v_5$ $v_6$ (5) | 6 6 3 | 13.5 |
| $v_{12}$ $v_{13}$ $v_{14}$ $v_{15}$ $v_{16}$ (5) | 4 5 5 1 | 16.5 |
| $v_7$ $v_8$ $v_9$ $v_{11}$ $v_{10}$ (5) | 3 5 4 3 | 18.5 |

Table 1: a) Topological analysis for the 1P-CNC direct graph $Z_{f=2}$ with $f = 2$ and $N = 45$ atoms (Figure 1a) grouped in 6 sets of symmetry-equivalent nodes having the same string $\{b_{ik}\}$ and therefore the same $w_i$ whose sum gives the Wiener index of the graph $W = 4865$; the sum $\sum b_{i1}$ gives twice the number of graph edges $B = 60$, $M = 10$. b) the case of the 1P-CNC dual graph $Z^*_{f=2}$ with $N^* = 16$ nodes divided in 4 orbits, $W = 255$, $B = 35$ $M = 4$. In both cases nodes are ranked from the minimal $\underline{w}$ to the maximal $\overline{w}$.

Lattice descriptor (3) allows to deal with the important concept of topological compactness. The most-compact structures are often seen as the chemically most stable ones. This statement implies a topological minimum principle on $W$: chemically stable molecular structures tend to minimize the lattice descriptor (3). The Wiener index behaves like a topological potential $\Xi^W = W$ operating on the chemical graph $G(N)$. We will analyze the action of $\Xi^W$ later.

Returning to the 1P-CNC graph with $f = 2$ and $N = 45$ (direct graph $Z_{f=2}$ in Figure 1a), the Table 1a summarizes the topological invariants for the 6 partitions (orbits) of the $N = 45$ nodes. It is worth to notice that the cardinality of all orbits in Table 1 is always a multiple of 5 reflecting the 5-fold symmetry of the nanocone induced by the pivotal pentagons at the apex. Atoms that share the minimum contribution $\underline{w} = \min\{w_i\} = 84.5$ to the formula (3), are called the minimal nodes $\underline{v}$ of the graph, i.e. the most nested vertices of $Z_{f=2}$. For $f = 2$ these are the five vertices of the pentagon (see Figure 1a). Conversely the ten external vertices with $\overline{w} = \max\{w_i\} = 128.5$ are the maximal nodes $\overline{v}$ of the graph corresponding to the less embedded nodes in $Z_{f=2}$. Similar data are reported in Table 1b for the dual representation $A^*_{f=2}$ of the 1P-CNC graph shown in Figure 1b (topological invariants of $Z^*_{f=2}$ will be marked by the starred superscript only in case of possible confusion). It is evident that the apical pentagon, being the minimal node with $\underline{w} = 12.5$, represents the more stable region also for $Z^*_{f=2}$. We will soon discover that these properties strongly depend from nanocone size $f$. Before investigating in which ways topological properties are affected by the size $f$, the following topological efficiency (or roundness) invariant $\rho$ needs to be introduced:

$$\rho = \frac{W}{N\underline{w}}, \quad \rho \geq 1, \tag{4}$$

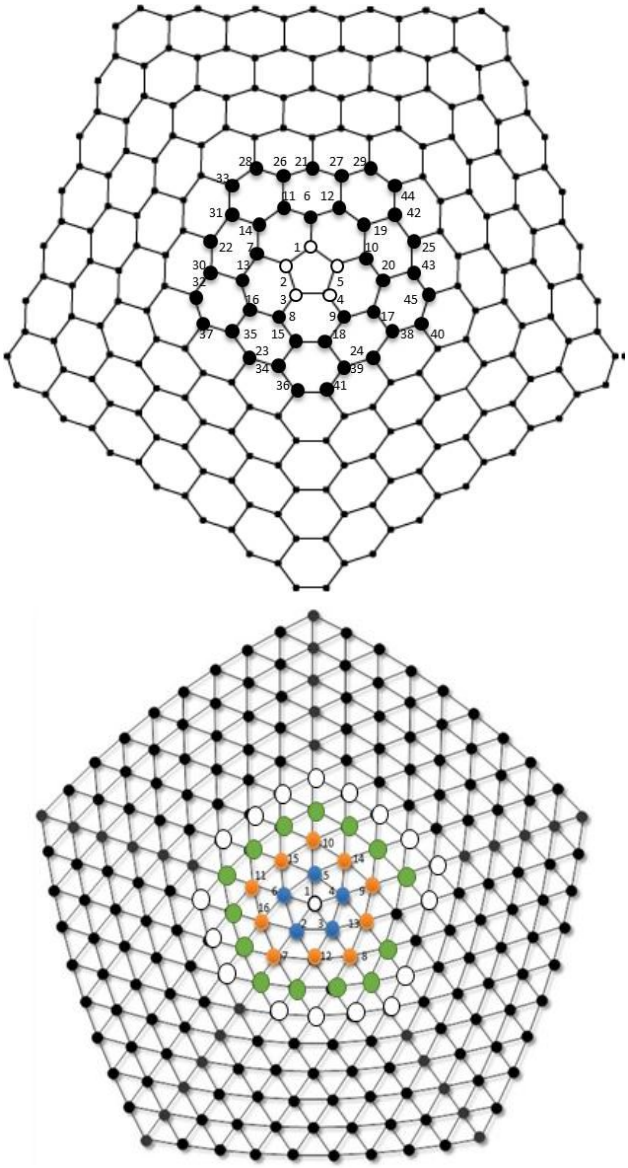

Figure 1: a) The structure of the 1P-CNC direct graph $Z_{f=2}$ with $f = 2$ and $N = 45$ atoms, five of them forming the central pentagon (white circles); b) the dual representation $Z^*_{f=2}$ of the same structure consists of N=16 nodes (numbered from 1 to 16). In this small dual nanocone the relative importance of the maximal nodes (the orange circles on the boundary) is clear. The structure with $f = 0$ corresponds in both graphs to the inner pentagon $P$ only. The $f = 1$ nanocone includes the first 5 hexagons around $P$; green balls indicate $Z^*_{f=3}$ perimeter and white circles the $Z^*_{f=4}$ one.

together with variant [12] the extreme topological efficiency (or roundness):

$$\rho^E = \frac{\overline{w}}{\underline{w}}, \quad \rho^E \geq 1. \tag{5}$$

Indices (4) and (5) can measure the global efficiency of a given graph $G$ in filling the space in the most compact way when compared to its minimal vertices $\underline{v}$ and they work quite well to identify the stable isomers, characterized by low values of $\rho$ and $\rho^E$, for many fullerenes and other carbon structures, see for example [13]. For graphs having all vertices "efficient" (i.e. with $WW$ close to $\underline{w}$) the resulting structure will be topologically compact (low $W$) and topologically round (low $\rho$ and $\rho^E$). In fact, during their growth, topologically efficient graphs keep their topological roundness indices (4,5) close to the lowest possible value 1. We therefore assume that also these two invariants operate on direct and dual chemical graphs as topological potentials $\Xi^\rho = \rho$ or $\Xi^{\rho^E} = \rho^E$ subject to a minimum principle like $\Xi^W$. As an example, for the two structures $Z_{f=2}$ and $Z^*_{f=2}$ represented in Figure 1, the respective efficiency indices are easily computed by formulae (4) and (5) using Table 1. That leads to the following determinations: $\rho = 1.279421$, $\rho^E = 1.520710$ for the direct and $\rho = 1.275$, $\rho^E = 1.48$ for the dual nanocone, both with $f = 2$ circles of hexagons around the pentagonal apex.

For the direct graph $Z_f$ consists of the pivotal pentagon $P$ surrounded by $f$ concentric belts of hexagons $f = 0, 1, 2, 3, \ldots\ldots$ the number of carbon atom $N$ and number of hexagons $n_6$ are connected to $f$ by the following formulas:

$$n_6 = \frac{5}{2}(f^2 + f) \tag{6}$$

$$N = 5 + 5(f^+ f). \tag{7}$$

For large lattices we then have $n \approx 5f^2$. Considering the presence of the central pentagon $n_5 = 1$, the total number of faces is $n_T = n_5 + n_6 = n_6 + 1$. By placing $f = 0$ in (6), the graph is reduced to the central pentagon with $n_T = n_5 = 1$ and $N = 5$. When the first hexagonal belt is completed $f = 1$, $n_T = 6$, $N = 20$ and so on. For dual nanocones the number of nodes $N^*$ corresponds, by definition, to the number of hexagonal rings plus the pivotal 5-star. From (6) it is therefore straightforward to derive the following rule for the number of nodes of the dual nanocone:

$$N^* = 1 + \frac{5}{2}(f^2 + f). \tag{8}$$

admitting $N^* \approx \frac{5}{2}f^2$ and $N^* \approx N/2$ asymptotic limits.

We end this short introduction to the formalism with an important observation about the "computability" of the topological invariants like $w_i$ and $W$ by formulas (2) and (3) for large structures like large $f$ nanocones. The answer has been provided for 1D infinite graphs in the early days of topological chemistry by the 1980 seminal paper [14] that shows the possibility to describe with polynomials of degree 3 the $W(N)$ curves for infinite graphs of conjugated polymers. This simple $W(N) \approx N^3$ scaling has been generalized [8] by the following rules that are conjectured to be valid, in the limit of large $N$, for any $D$-dimensional infinite lattices:

$$W \approx N^{(2D-1)/D} \tag{9}$$

$$w_i \approx N^{(D-1)/D}. \tag{10}$$

Similar relationships have been discovered for other lattice invariants, see the detailed investigations [15] that appeared in literature in recent years. In the next section the outcomes of the topological models presented above for both direct and dual nanocones will be used to derive interesting structural features about these peculiar "topological defects of the graphenic layers" in which the properties of a "multitude" of $n_6 = \frac{5}{2}(f^2 + f)$ hexagons (8) are deeply influenced by the presence of just one pentagon.

# 3 1P-CNC topological invariants

Table 2 presents the main topological invariants, derived from Equations (3,4,5) and related quantities, characterizing the direct graph $Z_f$ of the 1P-CNC nanocone scaling with $f$ up to 60 to build a structure with 59 belts of hexagons that surround the apical pentagon ($f = 0$). This $f = 60$ lattice includes 18.605 carbon atoms, quite far from the simulation capacity of today DFT computerized method. With a simple interpolation of Table 2 data, the following curve is derived for the Wiener index (3) of the direct nanocone $Z_f$:

$$W(f) = (124f^5 + 620f^4 + 1205f^3 + 1135f^2 + 516f + 90)/6. \tag{11}$$

The polynomial given in (11) provides the correct $W$ for all values of parameter $f \geq 0$, including the Wiener index of the isolated pentagon $W(0) = 15$ matching previously published results [16]. Equation (11), combined with (7) for $N(f)$, brings us to the curve :

$$W(N) = \frac{\sqrt{5}}{750}(25 - 175N + 124N^2)\sqrt{N}) \tag{12}$$

with asymptotic value:

$$W(N) = \frac{62}{375}\sqrt{5}N^{5/2} \quad \text{as} \quad N \to \infty \tag{13}$$

that contains the 5/2 exponent expected for nanosystems with $D = 2$ dimensionality, see Equations (9). The contribution to invariant (11) coming from the minimal node $\underline{w}(f)$ shows the proper power law:

$$\underline{w}(f) = (40f^3 + 87f^2 + 299f + 168)/12 \tag{14}$$

that produces for $\underline{w}(N)$, still using (7), the polynomial form of grade 3 in $n^{1/2}$:

$$\underline{w}(N) = \frac{2}{15}\sqrt{5}N^{3/2} - \frac{11}{20}N + \frac{49}{12}\sqrt{5}N^{1/2} - 7 \tag{15}$$

whose asymptotic form $\underline{w}(N)$ agrees to the one expected for 2D structures (10):

$$\underline{w}(N) \sim \frac{2}{15}\sqrt{5}N^{3/2} \quad \text{as} \quad N \to \infty. \tag{16}$$

Although the polynomial expressions (14,15) show the correct $N^{3/2}$ dependence, they reproduce the exact values for $\underline{w}$ only in limited intervals of parameter the $f$ that regulates the cone growth.

| $f$ | $N$ | $B$ | $M$ | $W$ | $\underline{w}$ | $\overline{w}$ | $\rho$ | $\rho^E$ |
|---|---|---|---|---|---|---|---|---|
| 0 | 5 | 5 | 2 | 15 | 3 | 3 | 1 | 1 |
| 1 | 20 | 25 | 6 | 615 | 24.5 | 34.5 | 1.255102 | 1.408163 |
| 2 | 45 | 60 | 10 | 4865 | 84.5 | 128.5 | 1.279421 | 1.52071 |
| 3 | 80 | 110 | 14 | 20790 | 203 | 319 | 1.280172 | 1.571429 |
| 4 | 125 | 175 | 18 | 63855 | 400 | 640 | 1.2771 | 1.6 |
| 5 | 180 | 255 | 22 | 159445 | 695.5 | 1125.5 | 1.273624 | 1.61826 |
| 6 | 245 | 350 | 26 | 345345 | 1109.5 | 1809.5 | 1.270456 | 1.630915 |
| 7 | 320 | 460 | 30 | 674220 | 1660 | 2726 | 1.269239 | 1.642169 |
| 8 | 405 | 585 | 34 | 1216095 | 2362 | 3909 | 1.271255 | 1.654953 |
| 9 | 500 | 725 | 38 | 2060835 | 3240.5 | 5392.5 | 1.271924 | 1.664095 |
| 10 | 605 | 880 | 42 | 3320625 | 4315.5 | 7210.5 | 1.271843 | 1.670838 |
| 11 | 720 | 1050 | 46 | 5132450 | 5602 | 9397 | 1.272475 | 1.677437 |
| 12 | 845 | 1235 | 50 | 7660575 | 7117 | 11986 | 1.273819 | 1.684137 |
| 13 | 980 | 1435 | 54 | 11099025 | 8886.5 | 15011.5 | 1.274465 | 1.689248 |
| 14 | 1125 | 1650 | 58 | 15674065 | 10930.5 | 18507.5 | 1.274645 | 1.693198 |
| 15 | 1280 | 1880 | 62 | 21646680 | 13269 | 22508 | 1.27451 | 1.696285 |
| 16 | 1445 | 2125 | 66 | 29315055 | 15922 | 27047 | 1.274164 | 1.698719 |
| 17 | 1620 | 2385 | 70 | 39017055 | 18909.5 | 32158.5 | 1.273677 | 1.700653 |
| 18 | 1805 | 2660 | 74 | 51132705 | 22251.5 | 37876.5 | 1.273099 | 1.7022 |
| 19 | 2000 | 2950 | 78 | 66086670 | 25955 | 44235 | 1.273101 | 1.704296 |
| 20 | 2205 | 3255 | 82 | 84350735 | 30045 | 51268 | 1.273234 | 1.706374 |
| 21 | 2420 | 3575 | 86 | 106446285 | 34547.5 | 59009.5 | 1.273206 | 1.708069 |
| 22 | 2645 | 3910 | 90 | 132946785 | 39482.5 | 67493.5 | 1.273056 | 1.709454 |
| 23 | 2880 | 4260 | 94 | 164480260 | 44850 | 76754 | 1.273382 | 1.711349 |
| 24 | 3125 | 4625 | 98 | 201731775 | 50685 | 86825 | 1.273635 | 1.713031 |
| 25 | 3380 | 5005 | 102 | 245445915 | 57010.5 | 97740.5 | 1.27375 | 1.71443 |
| 26 | 3645 | 5400 | 106 | 296429265 | 63846.5 | 109534.5 | 1.273757 | 1.715591 |
| 27 | 3920 | 5810 | 110 | 355552890 | 71213 | 122241 | 1.273676 | 1.716555 |
| 28 | 4205 | 6235 | 114 | 423754815 | 79130 | 135894 | 1.273525 | 1.717351 |
| 29 | 4500 | 6675 | 118 | 502042505 | 87617.5 | 150527.5 | 1.273319 | 1.718007 |
| 30 | 4805 | 7130 | 122 | 591495345 | 96692.5 | 166175.5 | 1.273108 | 1.718598 |
| 31 | 5120 | 7600 | 126 | 693267120 | 106350 | 182872 | 1.27319 | 1.71953 |
| 32 | 5445 | 8085 | 130 | 808588495 | 116636 | 200651 | 1.273201 | 1.720318 |
| 33 | 5780 | 8585 | 134 | 938769495 | 127570.5 | 219546.5 | 1.273154 | 1.720982 |
| 34 | 6125 | 9100 | 138 | 1085201985 | 139163.5 | 239592.5 | 1.273149 | 1.721662 |
| 35 | 6480 | 9630 | 142 | 1249362150 | 151420 | 260823 | 1.273298 | 1.722514 |
| 36 | 6845 | 10175 | 146 | 1432812975 | 164383 | 283272 | 1.273383 | 1.723244 |
| 37 | 7220 | 10735 | 150 | 1637206725 | 178072.5 | 306973.5 | 1.273414 | 1.723868 |
| 38 | 7605 | 11310 | 154 | 1864287425 | 192508.5 | 331961.5 | 1.273397 | 1.724399 |
| 39 | 8000 | 11900 | 158 | 2115893340 | 207711 | 358270 | 1.27334 | 1.724848 |
| 40 | 8405 | 12505 | 162 | 2393959455 | 223700 | 385933 | 1.273248 | 1.725226 |
| 41 | 8820 | 13125 | 166 | 2700519955 | 240495.5 | 414984.5 | 1.273127 | 1.72554 |
| 42 | 9245 | 13760 | 170 | 3037710705 | 258095.5 | 445458.5 | 1.27309 | 1.725944 |
| 43 | 9680 | 14410 | 174 | 3407771730 | 276521 | 477389 | 1.273113 | 1.726411 |
| 44 | 10125 | 15075 | 178 | 3813049695 | 295811 | 510810 | 1.273102 | 1.726812 |
| 45 | 10580 | 15755 | 182 | 4256000385 | 315985.5 | 545755.5 | 1.27306 | 1.727154 |
| 46 | 11045 | 16450 | 186 | 4739191185 | 337031.5 | 582259.5 | 1.273116 | 1.727612 |
| 47 | 11520 | 17160 | 190 | 5265303560 | 358988 | 620356 | 1.273184 | 1.728069 |
| 48 | 12005 | 17885 | 194 | 5837135535 | 381887 | 660079 | 1.273218 | 1.728467 |
| 49 | 12500 | 18625 | 198 | 6457604175 | 405748.5 | 701462.5 | 1.273223 | 1.728811 |
| 50 | 13005 | 19380 | 202 | 7129748065 | 430592.5 | 744540.5 | 1.273202 | 1.729107 |
| 51 | 13520 | 20150 | 206 | 7856729790 | 456439 | 789347 | 1.273158 | 1.729359 |
| 52 | 14045 | 20935 | 210 | 8641838415 | 483308 | 835916 | 1.273094 | 1.729572 |
| 53 | 14580 | 21735 | 214 | 9488491965 | 511219.5 | 884281.5 | 1.273011 | 1.729749 |
| 54 | 15125 | 22550 | 218 | 10400239905 | 540142.5 | 934477.5 | 1.273033 | 1.730057 |
| 55 | 15680 | 23380 | 222 | 11380765620 | 570144.0 | 986538.0 | 1.273037 | 1.730331 |
| 56 | 16245 | 24225 | 226 | 12433888895 | 601246.0 | 1040497.0 | 1.273020 | 1.730568 |
| 57 | 16820 | 25085 | 230 | 13563568395 | 633459.5 | 1096388.5 | 1.273002 | 1.730795 |
| 58 | 17405 | 25960 | 234 | 14773904145 | 666765.5 | 1154246.5 | 1.273058 | 1.731113 |
| 59 | 18000 | 26850 | 238 | 16069140010 | 701230.0 | 1214105.0 | 1.273092 | 1.731393 |
| 60 | 18605 | 27755 | 242 | 17453666175 | 736873.0 | 1275998.0 | 1.273105 | 1.731639 |
| 61 | 19220 | 28675 | 246 | 18932021625 | 773714.5 | 1339959.5 | 1.273101 | 1.731853 |
| 62 | 19845 | 29610 | 250 | 20508896625 | 811774.5 | 1406023.5 | 1.27308 | 1.732037 |
| 63 | 20480 | 30560 | 254 | 22189135200 | 851073.0 | 1474224.0 | 1.273045 | 1.732195 |
| 64 | 21125 | 31525 | 258 | 23977737615 | 891630.0 | 1544595.0 | 1.272995 | 1.732327 |
| 65 | 21780 | 32505 | 262 | 25879862855 | 933440.5 | 1617170.5 | 1.272968 | 1.732484 |
| 66 | 22445 | 33500 | 266 | 27900831105 | 976509.5 | 1691984.5 | 1.272978 | 1.732686 |
| 67 | 23120 | 34510 | 270 | 30046126230 | 1020895.0 | 1769071.0 | 1.272974 | 1.732863 |
| 68 | 23805 | 35535 | 274 | 32321398255 | 1066617.0 | 1848464.0 | 1.272956 | 1.733016 |
| 69 | 24500 | 36575 | 278 | 34732465845 | 1113655.5 | 1930197.5 | 1.272971 | 1.733209 |
| 70 | 25205 | 37630 | 282 | 37285318785 | 1162041.5 | 2014305.5 | 1.273003 | 1.73342 |

Table 2: Topological descriptors for direct nanocones $Z_f$ for $f = 0, 1, 2, \ldots, 60$ being $N(B)$ the number of nodes (bonds), $M$ the graph diameter, $W$ the Wiener index, $\underline{w}$ and $\overline{w}$ the WW of minimal and maximal vertices respectively, topological efficiency numbers $\rho$ and $\rho^E$. Lattice $f = 60$ includes 18.605 carbon atoms.

| $f$ | $N^*$ | $B^*$ | $M^*$ | $W^*$ | $\underline{w}^*$ | $\overline{w}^*$ | $\rho$ | $\rho^E$ |
|---|---|---|---|---|---|---|---|---|
| 0 | 1 | 0 | 0 | 0 | 0 | 0 | 1 | 1 |
| 1 | 6 | 10 | 2 | 20 | 2.5 | 3.5 | 1.333333 | 1.400000 |
| 2 | 16 | 35 | 4 | 255 | 12.5 | 18.5 | 1.275000 | 1.480000 |
| 3 | 31 | 75 | 6 | 1365 | 35.0 | 53.5 | 1.258065 | 1.528571 |
| 4 | 51 | 130 | 8 | 4785 | 74.5 | 117.0 | 1.259376 | 1.570470 |
| 5 | 76 | 200 | 10 | 13035 | 135.5 | 217.5 | 1.265780 | 1.605166 |
| 6 | 106 | 285 | 12 | 30030 | 223.5 | 363.5 | 1.267570 | 1.626398 |
| 7 | 141 | 385 | 14 | 61390 | 343.5 | 563.5 | 1.267511 | 1.640466 |
| 8 | 181 | 500 | 16 | 114750 | 499.0 | 826.0 | 1.270497 | 1.655311 |
| 9 | 226 | 630 | 18 | 200070 | 695.5 | 1159.5 | 1.272848 | 1.667146 |
| 10 | 276 | 775 | 20 | 329945 | 938.5 | 1572.5 | 1.273791 | 1.675546 |
| 11 | 331 | 935 | 22 | 519915 | 1233.0 | 2073.5 | 1.273917 | 1.681671 |
| 12 | 391 | 1110 | 24 | 788775 | 1584.0 | 2671.0 | 1.273565 | 1.686237 |
| 13 | 456 | 1300 | 26 | 1158885 | 1996.5 | 3373.5 | 1.272935 | 1.689707 |
| 14 | 526 | 1505 | 28 | 1656480 | 2475.5 | 4189.5 | 1.272148 | 1.692385 |
| 15 | 601 | 1725 | 30 | 2311980 | 3026.0 | 5127.5 | 1.271278 | 1.694481 |
| 16 | 681 | 1960 | 32 | 3160300 | 3649.0 | 6196.0 | 1.271766 | 1.697999 |
| 17 | 766 | 2210 | 34 | 4241160 | 4353.0 | 7403.5 | 1.271942 | 1.700781 |
| 18 | 856 | 2475 | 36 | 5599395 | 5143.0 | 8758.5 | 1.271894 | 1.702994 |
| 19 | 951 | 2755 | 38 | 7285265 | 6023.0 | 10269.5 | 1.271897 | 1.705047 |
| 20 | 1051 | 3050 | 40 | 9354765 | 6995.0 | 11945.0 | 1.272455 | 1.707648 |
| 21 | 1156 | 3360 | 42 | 11869935 | 8067.5 | 13793.5 | 1.272775 | 1.709761 |
| 22 | 1266 | 3685 | 44 | 14899170 | 9245.5 | 15823.5 | 1.272911 | 1.711481 |
| 23 | 1381 | 4025 | 46 | 18517530 | 10534.0 | 18043.5 | 1.272905 | 1.712882 |
| 24 | 1501 | 4380 | 48 | 22807050 | 11938.0 | 20462.0 | 1.272790 | 1.714022 |
| 25 | 1626 | 4750 | 50 | 27857050 | 13462.5 | 23087.5 | 1.272591 | 1.714949 |
| 26 | 1756 | 5135 | 52 | 33764445 | 15112.5 | 25928.5 | 1.272327 | 1.715699 |
| 27 | 1891 | 5535 | 54 | 40634055 | 16890.0 | 28993.5 | 1.272240 | 1.716607 |
| 28 | 2031 | 5950 | 56 | 48578915 | 18799.0 | 32291.0 | 1.272340 | 1.717698 |
| 29 | 2176 | 6380 | 58 | 57720585 | 20848.0 | 35829.5 | 1.272352 | 1.718606 |
| 30 | 2326 | 6825 | 60 | 68189460 | 23042.0 | 39617.5 | 1.272294 | 1.719360 |
| 31 | 2481 | 7285 | 62 | 80125080 | 25381.0 | 43663.5 | 1.272427 | 1.720322 |
| 32 | 2641 | 7760 | 64 | 93676440 | 27872.0 | 47976.0 | 1.272606 | 1.721297 |
| 33 | 2806 | 8250 | 66 | 109002300 | 30522.5 | 52563.5 | 1.272705 | 1.722123 |
| 34 | 2976 | 8755 | 68 | 126271495 | 33337.5 | 57434.5 | 1.272739 | 1.722820 |
| 35 | 3151 | 9275 | 70 | 145663245 | 36322.0 | 62597.5 | 1.272717 | 1.723405 |
| 36 | 3331 | 9810 | 72 | 167367465 | 39481.0 | 68061.0 | 1.272648 | 1.723893 |
| 37 | 3516 | 10360 | 74 | 191585075 | 42819.5 | 73833.5 | 1.272539 | 1.724296 |
| 38 | 3706 | 10925 | 76 | 218528310 | 46342.5 | 79923.5 | 1.272398 | 1.724626 |
| 39 | 3901 | 11505 | 78 | 248421030 | 50046.5 | 86339.5 | 1.272444 | 1.725186 |
| 40 | 4101 | 12100 | 80 | 281499030 | 53943.5 | 93090.0 | 1.272471 | 1.725694 |
| 41 | 4306 | 12710 | 82 | 318010350 | 58039.5 | 100183.5 | 1.272458 | 1.726126 |
| 42 | 4516 | 13335 | 84 | 358215585 | 62338.5 | 107628.5 | 1.272431 | 1.726517 |
| 43 | 4731 | 13975 | 86 | 402388195 | 66837.0 | 115433.5 | 1.272551 | 1.727090 |
| 44 | 4951 | 14630 | 88 | 450814815 | 71549.0 | 123607.0 | 1.272629 | 1.727585 |
| 45 | 5176 | 15300 | 90 | 503795565 | 76479.5 | 132157.5 | 1.272668 | 1.728012 |
| 46 | 5406 | 15985 | 92 | 561644360 | 81633.5 | 141093.5 | 1.272673 | 1.728377 |
| 47 | 5641 | 16685 | 94 | 624689220 | 87016.0 | 150423.5 | 1.272649 | 1.728688 |
| 48 | 5881 | 17400 | 96 | 693272580 | 92632.0 | 160156.0 | 1.272600 | 1.728949 |
| 49 | 6126 | 18130 | 98 | 767751600 | 98486.5 | 170299.5 | 1.272527 | 1.729166 |
| 50 | 6376 | 18875 | 100 | 848498475 | 104580.5 | 180862.5 | 1.272483 | 1.729409 |
| 51 | 6631 | 19635 | 102 | 935900745 | 110914.5 | 191853.5 | 1.272514 | 1.729742 |
| 52 | 6891 | 20410 | 104 | 1030361605 | 117501.5 | 203281.0 | 1.272518 | 1.730029 |
| 53 | 7156 | 21200 | 106 | 1132300215 | 124346.5 | 215153.5 | 1.272500 | 1.730274 |
| 54 | 7426 | 22005 | 108 | 1242152010 | 131447.5 | 227479.5 | 1.272528 | 1.730573 |
| 55 | 7701 | 22825 | 110 | 1360369010 | 138810.0 | 240267.5 | 1.272591 | 1.730909 |
| 56 | 7981 | 23660 | 112 | 1487420130 | 146445.0 | 253526.0 | 1.272629 | 1.731203 |
| 57 | 8266 | 24510 | 114 | 1623791490 | 154357.5 | 267263.5 | 1.272645 | 1.731458 |
| 58 | 8556 | 25375 | 116 | 1769986725 | 162552.5 | 281488.5 | 1.272640 | 1.731677 |
| 59 | 8851 | 26255 | 118 | 1926527295 | 171035.0 | 296209.5 | 1.272617 | 1.731865 |
| 60 | 9151 | 27150 | 120 | 2093952795 | 179810.0 | 311435.0 | 1.272578 | 1.732023 |
| 61 | 9456 | 28060 | 122 | 2272821265 | 188882.5 | 327173.5 | 1.272524 | 1.732154 |
| 62 | 9766 | 28985 | 124 | 2463709500 | 198246.0 | 343433.5 | 1.272531 | 1.73236 |
| 63 | 10081 | 29925 | 126 | 2667213360 | 207913.0 | 360223.5 | 1.272543 | 1.732568 |
| 64 | 10401 | 30880 | 128 | 2883948080 | 217892.0 | 377552.0 | 1.272539 | 1.732748 |
| 65 | 10726 | 31850 | 130 | 3114548580 | 228188.0 | 395427.5 | 1.27252 | 1.732902 |
| 66 | 11056 | 32835 | 132 | 3359669775 | 238790.5 | 413858.5 | 1.27257 | 1.733145 |
| 67 | 11391 | 33835 | 134 | 3619986885 | 249719.0 | 432853.5 | 1.272605 | 1.733362 |
| 68 | 11731 | 34850 | 136 | 3896195745 | 260979.0 | 452421.0 | 1.272624 | 1.733553 |
| 69 | 12076 | 35880 | 138 | 4189013115 | 272575.5 | 472569.5 | 1.272629 | 1.73372 |
| 70 | 12426 | 36925 | 140 | 4499176990 | 284513.5 | 493307.5 | 1.27262 | 1.733863 |

Table 3: Topological descriptors for dual nanocones $Z_f^*$ for $f = 0, 1, 2, \ldots, 60$ being $N^*(B^*)$ the number of graph vertices (edges), $M^*$ the dual graph diameter, $W^*$ the Wiener index, minimal and maximal $\underline{w}^*$ $\overline{w}^*$, $\rho$ and $\rho^E$. Size $f = 0$ corresponds to the graph with just one vertex (the dual pentagon) and no edges with $\rho = 1$ and $\rho^E = 1$ arbitrarily assigned values.

| $J$ | $f_J$ | $N^*$ | $w_P$ | $\underline{w}$ |
|---|---|---|---|---|
| 1 | 4 | 51 | 75.0 | 74.5 |
| 2 | 8 | 181 | 510 | 499.0 |
| 3 | 16 | 681 | 3740 | 3649.0 |
| 4 | 19 | 951 | 6175 | 6023.0 |
| 5 | 27 | 1891 | 17325 | 16890.0 |
| 6 | 31 | 2481 | 26040 | 25381.0 |
| 7 | 39 | 3901 | 51350 | 50046.5 |
| 8 | 42 | 4516 | 63962.5 | 62338.5 |
| 9 | 50 | 6376 | 107312.5 | 104580.5 |
| 10 | 54 | 7426 | 134887.5 | 131447.5 |
| 11 | 62 | 9766 | 203437.5 | 198246.0 |
| 12 | 66 | 11056 | 245052.5 | 238790.5 |

Table 4: The minimal node $\underline{v}$ migrates in the growing graph $Z_f^*$ of the dual nanocone with a characteristic bouncing path, with the $j$th-jump occurring when the graph reaches a critical dimension $f_J$. For the first 12 jumps ($J = 1, 2, \ldots, 12$) topological invariants for the graph $Z_f^*$ are reported being $\underline{w}$ ($w_P$) the contribution to Wiener index from the minimal node (the apical pentagon $R$). At size $f_J$ the minimal node $\underline{v}$ jumps on specific nodes of the hexagonal $J$th belt around $P$. Invariant $w_P(f_J) = 5/6 f_J^3 + 5/4 f_J^2 + 5/12 f_J$ obeys the exact cubic formula valid for 2D graphs.

Equation (11) for $W$ instead holds for any $f$. Formulae (14,15) are valid in the 8-steps range $11 \leq f \leq 18$ (Tables 2). If we consider for example the 4-steps interval $7 \leq f \leq 10$, the coefficients in Equation (14,15) need to be refitted and changed accordingly. This discontinuous size-effect on the $\underline{w}$ curve represents a pure topological effect that, due to the influence of $\underline{w}$ on the topological roundness invariants (4) and (5), causes a peculiar mechanism, early predicted in [8], consisting in the endless migration of the minimal nodes of the nanocone 1P-CNC occurring at precise values of the size parameter $f$, see Table 4 and Figures 3. The chemical implications induced by this migration of the nanocone properties are discussed in the next paragraph.

It is important to note here that, in general, quantities WW of formula (2) do not show any kind of discontinuous behavior. As an example of this fact we give the regular polynomial expression for the maximal nodes of the direct graph of the nanocone:

$$\overline{w}(N) = (68 f^3 + 171 f^2 + 139 f + 36)/12. \tag{17}$$

For every size $f$, expression (17) converges to the right $\overline{w}$ listed in Table 2. A perfect convergence also holds for relations $M(f) = 4f + 2$ and $B(f) = 15f^2 + 25f)/2 + 5$ giving, respectively, the values for the graph diameter and the number of bonds of $Z_f$.

Table 3 reports the lattice descriptors for the dual representation $Z_f^*$ of the 1P-CNC nanocone. Also in this case, the topological invariants allow a fast determination by polynomial and polynomial like curves with leading exponents depending only by the dimensionality of the system, in this case $D = 2$. For any $f \geq 0$, nanocone faces $n_T$ scale like $f^2$ (8), graph edges are $B^*(f) = (15f^2 + 5f)/2$. Graph diameter doubles $f$ with the exact formula $M^*(f) = 2f$ and for $N \to \infty$ it is half of the

analogous value of the direct graph $M^*(f) \approx M(f)/2$. The following interpolation formula is derived for the Wiener index:

$$W^*(f) = (62f^5 + 155f^4 + 160f^3 + 85f^2 + 18f)/24. \tag{18}$$

Also in this case, the Wiener index is correctly computed by (18) for all integer values $f \geq 0$, including the case of the graph made by the sole pentagon $W_{f=0} = 0$. From Equation (18) and (8), the polynomial-like curve of $N^{1/D}$ with grade $s = 2D + 1$ is obtained for $W^*(M)$:

$$W^*(N) = \frac{\sqrt{5}\sqrt{8N-3}}{750}(14 - 17N + 31N^2)\sqrt{N} \tag{19}$$

confirming the general rule (9) for 2D graph. Equation (20) admits the asymptotic trend:

$$W^*(N) \sim \frac{62}{375}\sqrt{\frac{5}{2}}N^{5/2} \quad \text{as} \quad N \to \infty. \tag{20}$$

We conclude this section devoted to the determination of the topological invariants of the 1P-CNC nanostructures by confirming that also $\underline{w}^*(f)$ is described by a set of cubic polynomials valid only in a limited range of $f$ (the same mechanism happened for (14) polynomial). On the contrary, the WW coming from the maximal nodes of $Z_f^*$ are represented by cubic form in $f$:

$$W^*(f) = (119f^3 + 126f^2 + 49f)/84 \tag{21}$$

with correct $f^{2D-1}$ scaling as $f \to \infty$. Equation (21), like (17), converges for every $f \geq 0$, see Table 3.

The exhaustive formalism presented in this section for the two graphs representing 1P-CNC will be used in the following to derive useful indications about nanocone stable configurations and the reactivity of its nodes. To keep our model as simple as possible, showing at the same time the high computational power of our topological tools, we will mainly analyze the topological properties of the nanocone by adopting the dual graph $Z_f^*$ picture.

# 4 Results and discussion

According to TM, the lattice invariants $W(N)$ (11) and $W(f)$ (18) act as the long-range topological potential $\Xi^W$ driving the nanosystem $G$ toward the most compact lattice configuration, whereas the topological potentials $\Xi^\rho$ and $\Xi^{\rho^E}$ (4,5) both privilege graph structures $G$ characterized by the presence of the extra-symmetry, the so-called topological roundness, which minimizes the set of WW gaps:

$$\|w_i - \underline{w}\| \to 0 \quad \forall i \in G. \tag{22}$$

Let's start by studying the Wiener index $W(N)$. The $\Xi^W$ influence on the growth of the nanocone has been intensively investigated in previous works [8,9] that present an original comparison between the nanocone $Z_f^*$ dual lattices and the dual graphene fragments $Gr^*$ with the same numbers of hexagonal rings $n_6$. In this case, after an initial substantial equivalence during the first steps of

the growth, the topological invariant $\Xi^W$ promotes the formation of 1P-CNC that shows in fact a Wiener index $W(Z^*_{n_6})$ lower than the corresponding value for the graphenic lattice:

$$(Z^*_{n_6}) < W(Gr^*_{n_6}). \tag{23}$$

We recall here that the number of hexagons $n_6$ and the number of hexagonal belts f are related by the Equation (6). The important result (23) points out two basal properties of the 1P-CNC nanosystem:

- 1P-CNC with size $n_6 \geq 500$ has a topological stability (probability of formation) comparable to the topological stability of graphenic fragments with the same number of hexagonal rings thanks to the higher topological compactness featured during its growth;
- This topological mechanism predicts therefore a non-negligible probability of finding fullerene-like fragments in graphene layers. This event has been experimentally observed [17] and the best theoretical explanation today for the appearance of these carbon structures in represented by the inequality (23).

Other important indications about the 1P-CNC growing mechanisms may be derived from the topological efficiency invariants (4,5) by setting $H^t(G) = \Xi^\rho$ searching for its local minima.

Extended calculations for $\rho$ and $\rho^E$ were performed in the $0 \leq f \leq 70$ size range; for $f = 70$ graphs $Z_f$ and$Z^*_f$ are composed, respectively, by 25.205 carbon atoms and 37.630 chemical bonds (for the direct lattice) and 12.425 hexagonal faces and one pentagon with 36.925 edges (dual lattice). These large numbers evidence the relevance of the TM sieve to quickly select meaningful configurations before using expensive quantum computations.

As discussed above, the two invariants $\underline{w}$ (14) and $\underline{w}^*$ present a peculiar non-converging behavior, just allowing numerical determination of $\rho$ and $\rho^E$ (4,5) by consecutive cubic polynomials are valid in limited intervals of $f$. Despite this minor complication, our simulations demonstrate that topological roundness carries an important amount of valuable information about nanocones structural properties and stability. This is immediately evident by observing the values listed in Table 3 in which the case $f = 0$ corresponds to the graph $Z^*_{f=0}$ with just one vertex (the isolated dual-pentagon) and no edges ($N = 1$, $B = 0$) with arbitrary unitary values for $\rho$ and $\rho^E$. Figure 2 represents the very interesting "oscillating" curve featured by the topological descriptor $\rho$ in the $2 \leq f \leq 70$ interval. It is important to notice here that, in the same range, the invariant $\rho^E$ produces instead a monotonic curve (see Table 3 values) without size-related effects. For this reason, the detailed study of the $\rho^E$ curves has not been considered in the present article.

By adopting $\rho$ as the topological potential $\Xi^\rho = \rho$ of the system, $H^t(G) = \Xi^\rho$ local minima, evidenced in Figure 2, correspond to nanocone stable structures that occur at special values of 1P-CNC size $f$. The absolute minimum $\rho_{\min} = 1.2581$ is attained for $f = 3$ when the third belt of hexagons is placed around the pivotal pentagon. The $Z^*_{f=3}$ nanocone results therefore a particularly stable system made by 26 dual vertices (Figure 1b). Structures with size in the range $4 \leq f \leq 11$ corresponds to a "repulsive barrier" in which the nanocone growth is opposed by the topological potential $\Xi^\rho$ that reaches its absolute maximum $\rho_{\max} = 1.2740$ for $f = 11$. The appearance of this barrier is chemically quite reasonable since for a small number of carbon atoms the system

tries to arrange itself by selecting chemically stable planar structures, like graphenic fragments or PAH's. By adding more hexagonal belts, the system evolves towards a relatively stable convex configuration for $15 \leq f \leq 19$ with a local minimum $\rho_{f=15} = 1.2713$, see the dotted rectangles in Figure 2. The presence of relatively stable nanocones is confirmed also for large $f$ values, see for example the point $\rho_{f=42} = 1.2724$ that corresponds to a direct nanocone with 42 belts of hexagons and a grand total of $N = 9245$ carbon atoms and $B = 13.760$ chemical bonds. Figure 2 shows the general behavior of the topological efficiency $\Xi^{\rho} = \rho$ for the $Z_f^*$ nanosystem and zooms on the local minima, e.g. the special sizes showing a relative stability like the magic values $f^* = 3, 15-19, 42, 50-54, 61-65$ evidenced in Figure 2 insets. The presence of preferred sizes $f^*$ individuate magic sizes that correspond to nanocones with a significant probability of formations that should be compared with the experimental structural investigations:

- The identification of these preferred configurations $f^* = 3, 15-19, 42, 50-54, 61-65$ represents a non-trivial finding of our models.

We complete the present topological study by presenting the second original result that unveils a relevant mechanism with big influences on nanocone chemistry. Our topological method shows in fact that:

- according with the proposed topological model, the minimal node of the nanocone changes its position in function of the size $f$ of the structure.

One has now to remember at this point that the minimal nodes $\underline{v}$ correspond to nodes with lowest contributions WW (2) and — in our approximation – with the highest chemical stability. For small cones, $\underline{v}$ it is located on the apex, e.g. it overlaps with the central pentagon $P$ (Figure 1b). When the dimension of the nanocone increases, this node migrates in the graph and follows a characteristic trajectory, shown in Figure 3, in which each jump corresponds to a specific number $f$ indicated here by the symbol $f_J$. The minimal node $\underline{v}$ makes a first jump (labeled by $J = 1$) to the next orbit when the nanocone structure includes 4 hexagonal belts, then $f_{J=1} = 4$; for simplicity we will use the symbol $f_1 = 4$. Initially, the minimal vertex coincides with the central pentagon $P$ of the structure, Figures 1 and 3. For $f = 1$, $N^* = 6$ its contribution $w_1 = w_P = \underline{w} = 2.5$ corresponds to the minimal WW value, and the same holds for $f = 2$ ($N^* = 16$, $\underline{w} = 12.5$) and $f = 3$ ($N^* = 31, \underline{w} = 35$). Then the jump from node $v_1$ to one of the five symmetric nodes $v_2$ to $v_6$ of the first orbit appears for $f = 4$, $N^* = 51$, $\underline{w} = 74.5$. That is when the pentagonal site becomes a less stable node with $w_P = 75$. Figure 3 shows the event $f_1$, the arrow shows that one of the 5 equivalent hexagons around $P$ becomes the stable node in the lattice. The next jump, bringing the minimal node to one of nodes $v_{12}$ to $v_{16}$ (as numbered in Figure 2) on the next orbit, appears in the next step $f = 8$, $N^* = 181$, $\underline{w} = 499$, $w_P = 510$. At this point the gap in the topological potential $(\underline{w} - w_P)$ exceeds 2% and this is a signal of the relative topological instability of the pentagon $P$ that then may be seen as a region with a certain chemical reactivity. When new concentric belts of hexagonal faces are added to the structure and the number of dual nodes reaches to $N^* = 681$, the minimal vertex makes a third, further jump, see step $f_3 = 16$ in Figure 3. Note that at jump threshold-size $f_J$ the minimal nodes lands into the hexagonal belt $f = J$. Obviously all five nodes around $P$ may be reached by the jumping node $\underline{v}$, so the reader must carefully consider all those symmetry-equivalent positions

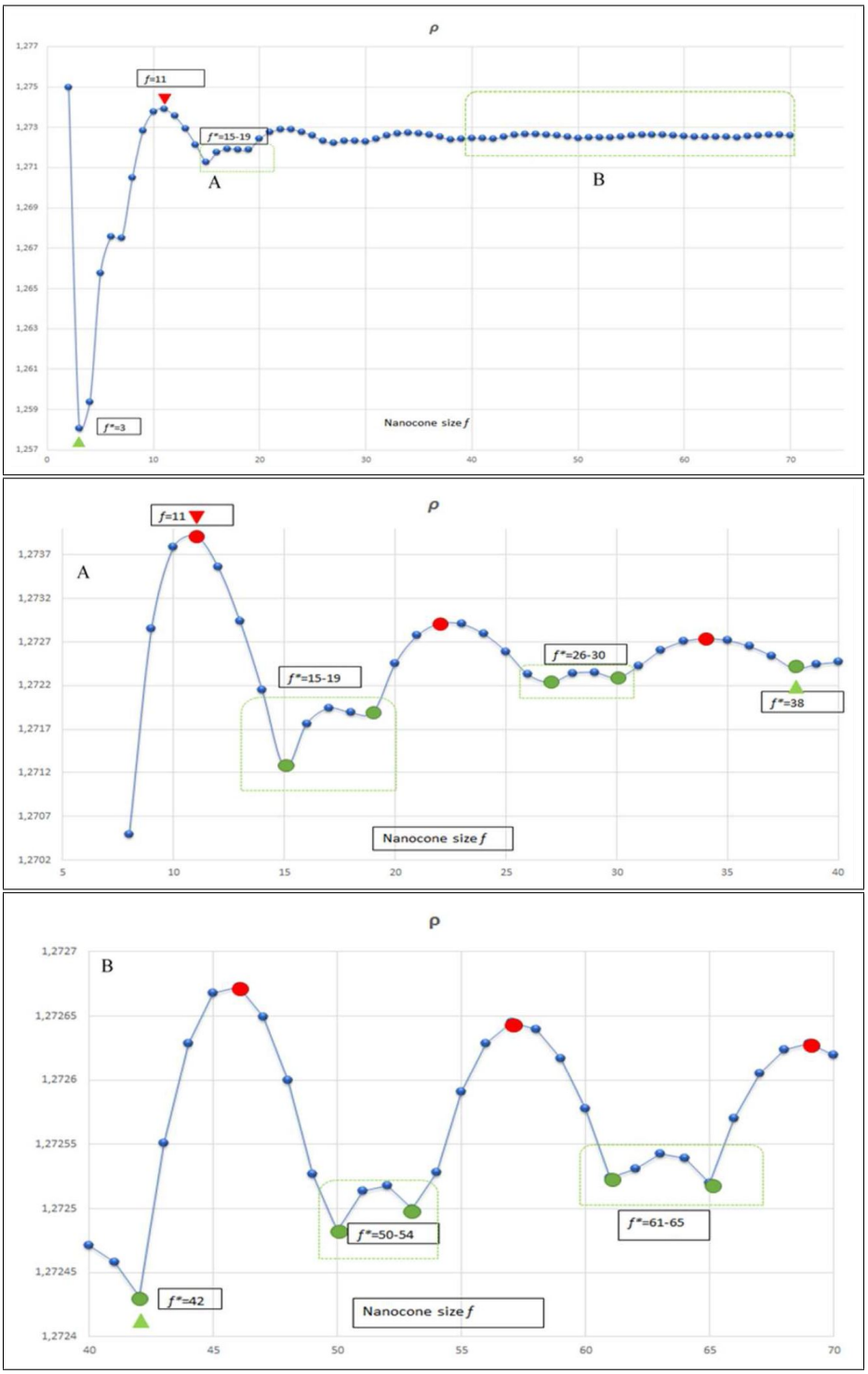


Figure 2: Topological roundness curve of the nanocone 1P-CNC in its dual representation $Z_f^*$ for $2 \leq f \leq 70$. Green and orange triangles signal the two stable-most sizes $f^* = 3, 15$ whereas the red one points to the most unstable cone with $f = 11$. The insets show other typical local minima corresponding to other magic sizes $f^* = 42, 50-54, 61-65$. Case $f = 3$ corresponds to the graph made by the pentagon with 3 concentric belts of hexagons.

that are neglected in our illustrations to keep the graphics as simple as possible. For example, Figure 3 shows two of the equivalent nodes that may host the minimal node $\underline{v}$ at the third jump being $f_3 = 16$ the threshold-size triggering that jump. By increasing $f$, the minimal vertices $\underline{v}$ drift away from the central pentagon $P$ while moving to the next orbit. Table 4 shows, in terms of the nanocone size, the endless steps driving $\underline{v}$ from the central pentagonal face toward the periphery of the nanocone along a peculiar path that skips the five 6-ribs of the graph $Z_f^*$ (see Figure 3), confirming in this way the early results [8,11c] and what we believed is the main prediction arising from the topological approach:

- Topological model envisions an original topological mechanism which migrates the minimal node in the dual graph during the growth of the graph itself.

From the chemical point of view the above original finding provides some grounds to a chemically reactive apex for large nanocone. Quite a meaningful prediction, rich of practical and theoretical implications, coming from considering non-local topological interactions (2). Nanotube tips, that presents extended rearrangements of the $sp^2$ carbon atoms network, have recently attracted considerable attention as possible electron emitters [18]. Present results point out that electronic properties of $sp^2$ carbon systems are deeply rooted in the topology of their atomic network. Configurations depicted in Figures 2 and 3 deserve therefore deeper ab initio investigation, being the principal goal of the topological tools described above a fast way to individuate meaningful nanostructures worth of successive experimental and theoretical studies.

# 5 Summary and outlook

This article applies the topological modeling approach, already presented in literature, which looks to a chemical carbon structures with $N$ atoms (like graphene or nanocones) like cubic graphs made by $N$ nodes of degree 3 that evolves under the effect of the topological potential $H^t(G) = \Xi^\rho$ that coincides with the topological efficiency (roundness) of the system. This "crude" approximation produces, once applied to the nanocone 1P-CNC in its dual representation, interesting theoretical conclusions in a negligible amount of computational time. In such a way, new chemical mechanisms influencing the chemical relative stability and the probability of formation of such nanostructures have been originally predicted and should be deeply investigated in the future with quantum-mechanical investigations. Two peculiar phenomena arising as pure topological features of the nanocone topological long-distance connectivity are reported above: (i) 1P-CNC presents peculiar magic sizes $f^*$ corresponding to $\Xi^\rho$ local minima making the existence of this nanostructure more probable; (ii) the pivotal pentagon is expected to become more and more reactive (or topologically unstable) by increasing lattice size $f$. Ab-initio investigations are required to confirm these predictions.

We aim ending this article by quoting Slatter's sentence [18] on the role of system dimensionality D in nanocone: "... Carbon cones are peculiar mesoscopic objects. They are characterized by a continuous transition from fullerene to graphite through a tubular-like intermedium. The dimensionality changes gradually as the cone opens. It resembles a 0-D cluster at the apex, then proceeds to a 1-D 'pipe' and finally approaches a 2-D layer. The carbon cones may have complex

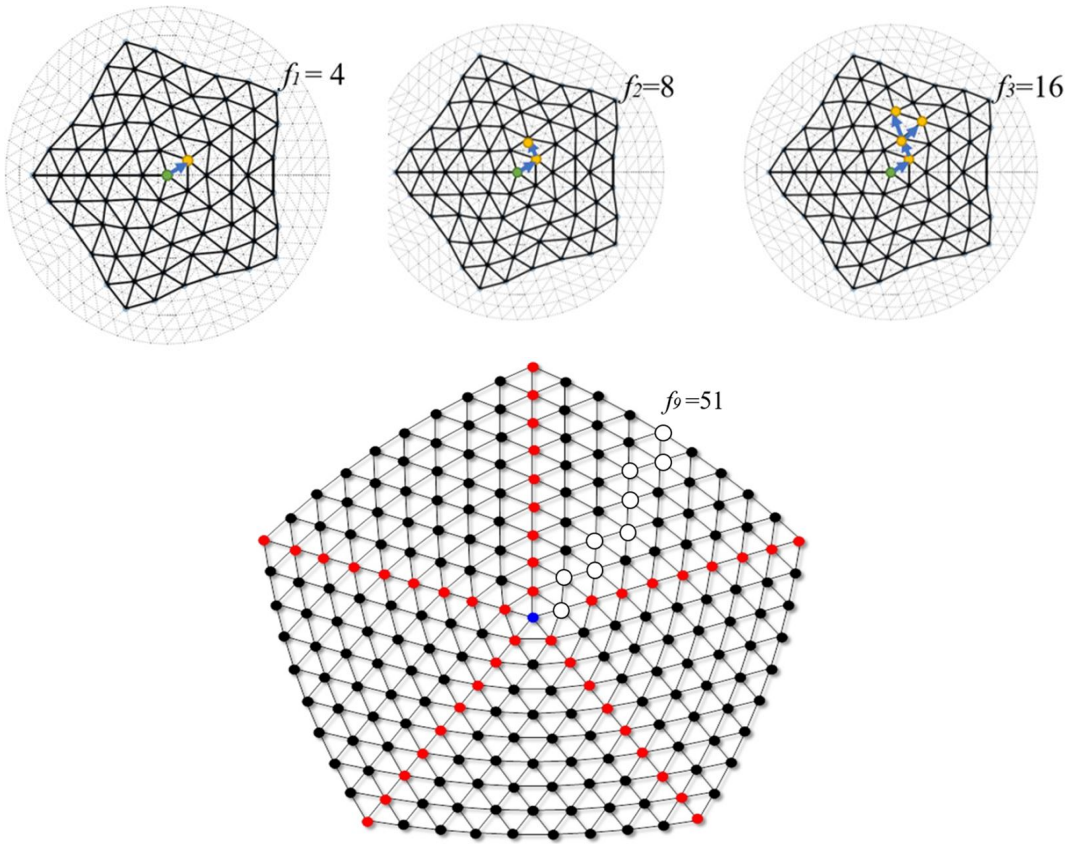


Figure 3: Topological migration of the minimal vertex in the dual nanocone 1P-CNC $Z_f^*$. The first jumps $f_1, f_2, f_3$, are shown by the blue arrows. The case $f_3$ remembers the presence of symmetry equivalent nodes in the fivefold structure of the graphs. An example of a jump occurring in large cone $f_9$ is given, the v migration path being evidenced by the white circles.

band structures and fascinating charge transport properties, from insulating at the apex to metallic at the base. They might be used as building units in future nanoscale electronics devices". As shown above by our results, system dimensionality $D$ plays a key-role in the topological modeling methods with possible fruitful applications to other $sp^2$ and $sp^3$ chemical infinite systems.

# References


[1] Ge, M. and Sattler, K., 1994. Observation of fullerene cones. *Chemical physics letters*, 220(3-5), pp.192-196.

[2] a) Cataldo, F., Putz, M.V., Ursini, O., Hafez, Y. and Iglesias-Groth, S., 2015. On the action of ozone on Single-Wall Carbon Nanohorns (SWCNH). *Fullerenes, Nanotubes and Carbon Nanostructures*, 23(12), pp.1095-1102. b) Valentini, F., Ciambella, E., Boaretto, A., Rizzitelli, G., Carbone, M., Conte, V., Cataldo, F., Russo, V., Casari, C.S., Chillura-Martino, D.F. and Caponetti, E., 2016. Sensor Properties of Pristine and Functionalized Carbon Nanohorns. *Electroanalysis* 28(10):2489-2499.

[3] Charlier J.-C. and Rignanese, G.-M., 2001. Electronic Structure of Carbon Nanocones 86(26) *Phusical Review Letters* 2001, 5970-5973

[4] De Souza, A.L., Da Silva Jr, A.M., Dos Santos, H.L. and De Almeida, W.B., 2017. Oxidized single-walled carbon nanotubes and nanocones: a DFT study *RSC Adv.*, 2017, 7, 13212 DOI: 10.1039/c7ra00301c

[5] Guerra, J., Herrero, M.A. and Vázquez, E., 2014. Carbon nanohorns as alternative gene delivery vectors. *RSC Advances*, 4(52), pp.27315-27321.

[6] Schwerdtfeger, P., Wirz, L.N. and Avery, J., 2015. The topology of fullerenes. *Wiley Interdisciplinary Reviews: Computational Molecular Science*, 5(1), pp.96-145.

[7] Karousis, N., Suarez-Martinez, I., Ewels, C.P. and Tagmatarchis, N., 2016. Structure, properties, functionalization, and applications of carbon nanohorns. *Chemical reviews*, 116(8), pp.4850-4883.

[8] Cataldo, F., Ori, O. and Iglesias-Groth, S., 2010. Topological lattice descriptors of graphene sheets with fullerene-like nanostructures, *Molecular Simulation*, 36:5, 341-353.

[9] Cataldo, F., Ori, O., Graovac, A., 2013. Graphene topological modifications, in: M. V. Putz (Ed.), *Advances in Chemical Modeling* (Chemistry Research and Applications, Vol. 3) Nova, New York, pp. 241–260.

[10] Balaban A.T., Klein J. and Liu X., 1994. Graphitic cones *Carbon* 32(2), 357-359.

[11] a) Alipour, M.A. and Ashrafi, A.R., 2009. Computer Calculation Of The Wiener Index Of One-Pentagonal Carbon Nanocone. *Digest Journal of Nanomaterials & Biostructures* (DJNB), 4(1). b) Khalifeh, M.H., Yousefi-Azari, H. and Ashrafi, A.R., 2010. A method for computing the Wiener index of one-pentagonal carbon nanocones. *Current Nanoscience*, 6(2), pp.155-157. c) Koorepazan-Moftakhar, F., R Ashrafi, A., Ori, O. and V Putz, M., 2015. Topological invariants of

nanocones and fullerenes. *Current Organic Chemistry*, 19(3), pp.240-248.

[12] a) Schwerdtfeger P, Wirz L, Avery J., 2013. Program fullerene: a software package for constructing and analyzing structures of regular fullerenes. *J Comput Chem.* 34:1508–1526. doi: 10.1002/jcc.23278. b) Extreme topological efficiency index has $\rho^E$ been introduced by Prof. D. Vukicevic, Split University, Croatia http://mapmf.pmfst.unist.hr/˜vukicevi/ as a modification of $\rho$, 2010.

[13] a) Vukicevic, D., Cataldo, F., Ori, O. and Graovac, A., 2011. Topological efficiency of C66 fullerene. *Chemical physics letters*, 501(4), pp.442-445. b) Graovac, A., Ashrafi, A.R. and Ori, O., 2014. Topological efficiency approach to fullerene stability–Case study with $C_{50}$. *Advances in Mathematical Chemistry and Applications*, 2, pp.3-23. c) Ori, O., Cataldo, F., Vukičević, D. and Graovac, A., 2011. Topological Determination of 13C–NMR Spectra of $C_{66}$ Fullerenes. In *The Mathematics and Topology of Fullerenes* (pp. 205-216). Springer Netherlands. d) De Corato, M., Benedek, G., Ori, O. and Putz, M.V., 2012. Topological study of schwarzitic junctions in 1D lattices. International *Journal of Chemical Modeling*, 4(2/3), p.105. e) Bumbacila, B., Ori, O. , Cataldo, F., and Putz, M.V., 2017. Topological Modeling of Carbon Nano-lattices. *Current Organic Chemistry*, 21(27), p.1-14.

[14] Bonchev, D. and Mekenyan, O., 1980. A Topological Approach To The Calculation Of The $\pi$-Electron Energy And Energy Gap of Infinite Conjugated Polimers, *Z.Naturforsch.*, 35a, 739-747.

[15] a) Kaatz, F.H. and Bultheel, A., 2015. Dimensionality of hypercube clusters. *J. Math. Chem.*, 54(1):33-43, 2016. b) Kaatz, F.H. and Bultheel, A., 2015. Topological indices for nanoclusters. *Comput. Mater. Sci.*, 99:73-80. c) Kaatz, F.H. and Bultheel, A., 2014. Informational thermodynamic model for nanostructures. *J. Math. Chem.*, 52(6):1563-1575. d)Kaatz, F.H. and Bultheel, A., 2013. Power law statistics of rippled graphene nanoflakes. *J. Math. Chem.*, 51(5):1221-1230. e) Kaatz, F.H. and Bultheel, A., 2013. Statistical properties of carbon nanostructures. *J. Math. Chem.*, 51(5):1211-1220.

[16] Ashrafi, A.R. and Mohammad-Abadi, Z., 2012. The Wiener index of one-pentagonal carbon nanocone. *Fullerenes, Nanotubes and Carbon Nanostructures*, 20(8), pp.688-695.

[17] Cataldo, F., 2002. The impact of fullerene-like concept in carbon black science, *Carbon* 40, pp. 157–162.

[18] Sattler, K., 1995. Scanning tunneling microscopy of carbon nanotubes and nanocones. *Carbon*, 33(7), pp.915-920.

[19] Ori, O., Cataldo, F., Putz, M.V., Kaatz, F. and Bultheel, A., 2016. Cooperative topological accumulation of vacancies in honeycomb lattices. *Fullerenes, Nanotubes and Carbon Nanostructures*, 24(6), pp.353-362.

[20] Sabirov, D.S., Ori, O. and László, I., 2018. Isomers of the C84 fullerene: a theoretical consideration within energetic, structural, and topological approaches. *Fullerenes, Nanotubes and Carbon Nanostructures*, (just-accepted). https://doi.org/10.1080/1536383X.2017.1405389

[21] Ori, O., Cataldo, F. and Graovac, A., 2009. Topological ranking of $C_{28}$ fullerenes reactivity. *Fullerenes, Nanotubes and Carbon Nanostructures*, 17(3), pp.308-323.